JOURNAL OF MATERIALS SCIENCE 22 (1987) 3261–3264

Novel solid solution precursor method for the preparation of ultrafine Ni–Zn ferrites

P. RAVINDRANATHAN, K. C. PATIL
Department of Inorganic and Physical Chemistry, Indian Institute of Science, Bangalore 560012, India

Ultrafine Ni–Zn ferrites, $Ni_xZn_{1-x}Fe_2O_4$, have been prepared by the thermal decomposition/combustion of novel solid solution precursors of the type, $(N_2H_5)_3Ni_xZn_{1-x}Fe_2(N_2H_3COO)_9 \cdot 3H_2O$ where x = 0.2 to 0.8. The novelty of the precursors being their low temperature, exothermic, gas producing self-sustained decomposition. Fine particle nature of the ferrites has been indicated by X-ray powder diffraction, transmission electron microscopy and surface area measurements. Fine particle Ni–Zn ferrites sinter at 1000° C, 24 h to achieve almost 99% theoretical density.

1. Introduction

Nickel zinc ferrites, $Ni_xZn_{1-x}Fe_2O_4$ have been of interest because of their technological applications [1–4] in antenna rods, high frequency inductors and transformer cores, read/write heads for high speed digital tape or disc recordings etc. It is essential that the recording head material should have high density to give good wear properties against the rapidly moving tapes with their abrasive coating of iron oxide [5]. The magnetic properties of the ferrite are determined by chemical composition, porosity, grain size and microstructure. The recent developments in the preparation of Ni–Zn ferrites by wet chemical methods and hot pressing have been discussed [4]. Presently, we report the preparation of ultrafine Ni–Zn ferrites by extending the solid solution precursor technique [6, 7] used for the preparation of ultrafine ferrites, MFe_2O_4 where M = Mg, Mn, Co, Ni and Zn. The characterization of fine particle nature of $Ni_xZn_{1-x}Fe_2O_4$, where x = 0.2 to 0.8 has been made by X-ray powder diffraction (XRD), transmission electron microscopy (TEM) and surface area measurements. The magnetic properties, microstructure and sintering studies of fine particle Ni–Zn ferrites have also been investigated.

2. Experimental procedure

Aqueous solutions of metal sulphates of nickel, zinc and iron(II) in the required ratio were mixed and a solution of N_2H_3COOH in $N_2H_4 \cdot H_2O$ was added until the precipitate formed initially dissolved [8]. Bluish pink crystalline solids separated from the solution kept exposed to air, in a couple of days. The crystals were washed with alcohol, ether and dried over P_2O_5 in a vacuum desiccator. The composition of the crystals were fixed to be $(N_2H_5)_3Ni_xZn_{1-x}Fe_2(N_2H_3COO)_9 \cdot 3H_2O$ where x = 0.2, 0.4, 0.5, 0.6 and 0.8 by chemical analysis (Table I). The iron content in the precursor was determined gravimetrically as Fe_2O_3 after separation as iron cupferrate complex. Nickel and zinc were separated and estimated by EDTA titrations [9, 10]. Hydrazine content was determined volumetrically using 0.025 M KIO_3 solution under Andrews conditions [10].

2.1. Physical measurements

Infrared spectra of the precursors were recorded as nujol mulls using a Perkin Elmer 781 spectrophotometer. Simultaneous thermogravimetry–derivative thermogravimetry–differential thermal analysis (TG–DTG–DTA) of the samples were recorded using an Ulvac Sinku-Riko TA 1500 instrument. All the experiments were carried out under ambient conditions using 5 to 6 mg samples in a platinum cup. The heating rate employed was 20° C min^{-1}. X-ray powder diffraction (XRD) patterns of the precursors and $Ni_xZn_{1-x}Fe_2O_4$ were recorded on a Philips PW 1050/70 diffractometer using Co$K\alpha$ radiation. Brunauer–Emmett–Teller surface areas of the ferrites were

TABLE I Chemical analysis data of $(N_2H_5)_3Ni_xZn_{1-x}Fe_2(N_2H_3COO)_9 \cdot 3H_2O$

x	% Ni		% Zn		% Fe		% of hydrazine	
	Obsd *	Theor.†	Obsd	Theor.	Obsd	Theor.	Obsd	Theor.
0.2	1.11	1.17	5.16	5.21	11.09	11.13	38.21	38.26
0.4	2.24	2.34	3.90	3.91	11.10	11.14	38.28	38.31
0.5	2.89	2.93	3.15	3.26	11.07	11.15	38.30	38.33
0.6	3.43	3.52	2.64	2.61	11.02	11.16	38.31	38.36
0.8	4.65	4.70	1.24	1.31	11.08	11.17	38.40	38.41

*Observed.
†Theoretical

0022–2461/87 $03.00 + .12

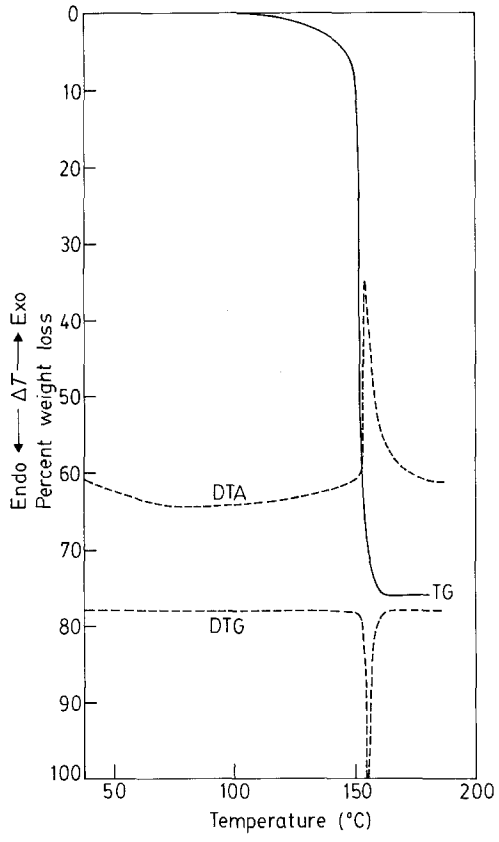

Figure 1 Simultaneous TG–DTG–DTA of $(N_2H_5)_3Ni_{0.5}Zn_{0.5}Fe_2(N_2H_3COO)_9 \cdot 3H_2O$.

measured by nitrogen adsorption using a Micromeritics Accusorb 2100E instrument. A vibrating sample magnetometer (EG and G Princeton Applied Research, MODEL 155) was used to determine the saturation magnetization of the ferrites at room temperature. The green ferrites were pelletized using polyvinyl alcohol (1%) as binder and the pellets were sintered at desired temperatures and times. The densities of sintered products were determined using a pyknometer.

3. Results and discussion

3.1. Characterization of precursors

The results of the chemical analysis (Table I) correspond to the formula $(N_2H_5)_3Ni_xZn_{1-x}Fe_2(N_2H_3COO)_3 \cdot 3H_2O$, $x = 0.2$ to 0.8. Infrared spectra of the complexes are similar to those of $N_2H_5M(N_2H_3COO)_3 \cdot H_2O$ where M = Fe, Ni and Zn and show characteristic N–N stretching frequencies of $N_2H_5^+$ and $N_2H_3COO^-$ ions at 965 and 990 cm^{-1} respectively [11, 12].

X-ray powder diffraction patterns of the precursors reveal that the complexes are isostructural possessing monoclinic structure of $N_2H_5Fe(N_2H_3COO)_3 \cdot H_2O$ [13]. The unit cell dimensions (Table II) clearly reveal that solid solutions of the type $(N_2H_5)_3Ni_xZn_{1-x}Fe_2(N_2H_3COO)_9 \cdot 3H_2O$ are formed in the entire range of $x = 0.2$ to 0.8.

Thermal decomposition studies of the precursors show that all the complexes decompose exothermically in a single step in the temperature range 120 to 220° C. The results of TG-DTA of the complexes are summarized in Table III and a typical thermogram is shown in Fig. 1. It can be observed that the weight loss in TG corresponds to the formation of corresponding Ni–Zn ferrite, $Ni_xZn_{1-x}Fe_2O_4$. The combustion of nickel zinc iron complexes is similar to that observed for metal hydrazine carboxylates [8]. The combustion is autocatalytic once ignited and leaves behind voluminous Ni–Zn ferrites.

3.2. Characterization of fine particle Ni–Zn ferrites

The results of XRD, magnetic and surface area measurements of fine particle Ni–Zn ferrites are summarized in Table IV. Formation of Ni–Zn ferrite by the thermal decomposition of the precursors was confirmed by X-ray powder diffraction patterns [14] of the residues (Fig. 2). The diffractograph shows a very broad line, indicating fine particle nature of the

TABLE II Unit cell dimensions for the monoclinic $(N_2H_5)_3Ni_xZn_{1-x}Fe_2(N_2H_3COO)_9 \cdot 3H_2O$

x	a (nm)	b (nm)	c (nm)	β°
0.0	1.2130	1.1006	1.0279	120.73
0.2	1.2140	1.1043	1.0280	121.09
0.4	1.2146	1.0971	1.0267	121.09
0.5	1.2155	1.1012	1.1271	121.09
0.6	1.3151	1.1916	1.1116	121.03
0.8	1.2174	1.0949	1.0275	121.03
1.0	1.2111	1.1016	1.0268	121.53

TABLE III Thermal analysis data of $(N_2H_5)_3Ni_xZn_{1-x}Fe_2(N_2H_3COO)_9 \cdot 3H_2O$

x	Thermogravimetry			DTA peak* temperature (° C)	Products
	Temperature range (° C)	% Final wt. loss			
		Observed	Theoretical		
0.2	130–170	76.05	76.12	150	$Ni_{0.2}Zn_{0.8}Fe_2O_4$
0.4	140–220	76.20	76.22	150, 210	$Ni_{0.4}Zn_{0.6}Fe_2O_4$
0.5	120–165	76.10	76.27	155	$Ni_{0.5}Zn_{0.5}Fe_2O_4$
0.6	140–165	76.25	76.32	145	$Ni_{0.6}Zn_{0.4}Fe_2O_4$
0.8	140–170	76.30	76.42	143	$Ni_{0.8}Zn_{0.2}Fe_2O_4$

*All DTA peaks are exothermic.

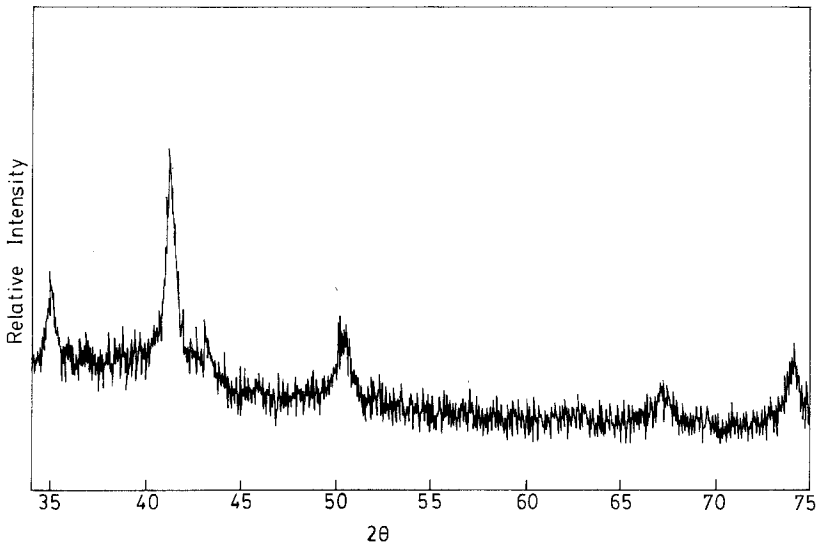

Figure 2 X-ray powder diffraction pattern of green $Ni_{0.5}Zn_{0.5}Fe_2O_4$.

ferrites. The lattice constant, a of Ni–Zn ferrites [15] decreases linearly as a function of concentration of nickel as seen from Fig. 3. The average crystallite sizes of $Ni_xZn_{1-x}Fe_2O_4$ calculated from the X-ray line broadening [16] are found to be in the range of 10 to 14 nm.

The BET surface area of the green Ni–Zn ferrites varies from 42 to 104 m^2g^{-1} (Table IV). These values are inbetween those of $NiFe_2O_4$ (26 m^2g^{-1}) and $ZnFe_2O_4$ (108 m^2g^{-1}) prepared by the solid solution precursors $N_2H_5M_{1/3}Fe_{2/3}(N_2H_3COO)_3 \cdot H_2O$ where M = Ni and Zn respectively [6]. The observed decrease in surface area values of Ni–Zn ferrites as the concentration of nickel (x) increases is due to the sintering. The combustion of nickel complex, $N_2H_5Ni(N_2H_3COO)_3 \cdot H_2O$, always takes place with shrinking rather than swelling as seen in other metal hydrazinecarboxylates. The exact reason for this behaviour of metal complex is not clear.

The magnetization curves (M–H curve) of Ni–Zn ferrites at room temperature are characterized by having zero remanance and coercivity and the ferrites are super-paramagnetic in nature [17]. The green ferrites prepared at 250° C does not attain saturation magnetization even at 18 K Oersted. However, the green Ni–Zn ferrites were pelletized and heated for 24 h at 900° C to increase the particle size thus rendering them suitable for saturation magnetization measurements. The values for various compositions are given in Table IV. As expected the magnetic moment reaches a maximum value of 70 emu g^{-1} at $x = 0.5$. This may be due to the preference of nickel ions for octahedral sites whereas zinc ions exclusively select tetrahedral sites making the saturation moment to be a function of zinc content [15].

Fine particle Ni–Zn ferrites have been sintered at 800, 900, 1000 and 1100° C for 24 h. About 99.5% of the theoretical density was achieved for all the ferrites at 1100° C. A typical density against temperature plot is given in Fig. 4. Increased reactivity of the fine particles is responsible for achieving almost theoretical density ferrites at low temperatures compared to those normally employed ($\geqslant$ 1200° C). Typical electron micrograph of $Ni_{0.5}Zn_{0.5}Fe_2O_4$ ferrites prepared at 250° C is shown in Fig. 5. The particle size calculated from the TEM is $\sim$ 60 nm. Typical scanning electron micrograph of $Ni_{0.5}Zn_{0.5}Fe_2O_4$ sintered at 1000° C is shown in Fig. 6 which show the microstructure and the grain size to be very small ($< 3\,\mu m$).

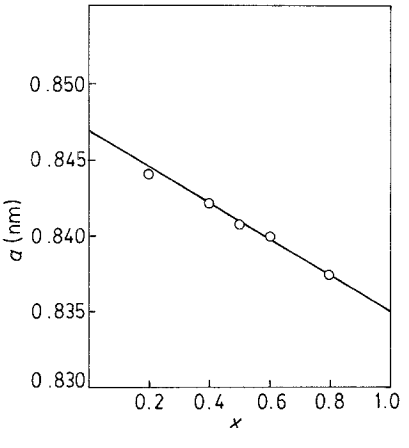

Figure 3 Variation of lattice constant a as a function of x in $Ni_xZn_{1-x}Fe_2O_4$.

3.3. Mechanism

Formation of fine particle Ni–Zn ferrites by the thermal decomposition/combustion of solid solution precursors like, $(N_2H_5)_3Ni_xZn_{1-x}Fe_2(N_2H_3COO)_9 \cdot 3H_2O$ can be attributed to their low temperature, exothermic, gas producing self-sustained decomposition. Evolution of large amounts of gases like NH_3, H_2O, CO_2 and N_2 facilitate formation of small particle, large surface area $Ni_xZn_{1-x}Fe_2O_4$ by dissipating the heat and reducing sintering of the product.

TABLE IV Some properties of Ni–Zn ferrites, $Ni_xZn_{1-x}Fe_2O_4$

x	Crystallite size from XRD (nm)	Surface Area (m^2g^{-1})	Saturation magnetization at 23° C (emu g^{-1})
0.2	11	104	55
0.4	10	100	64
0.5	12	72	70
0.6	14	53	69
0.8	14	42	61

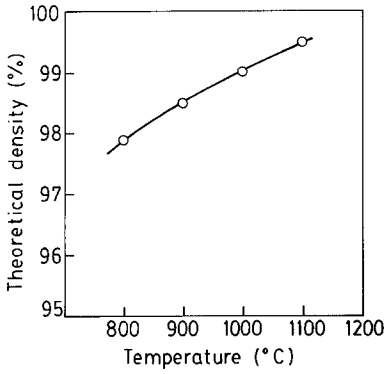

Figure 4 Plot of theoretical density (%) as a function of sintering temperature for $Ni_{0.5}Zn_{0.5}Fe_2O_4$.

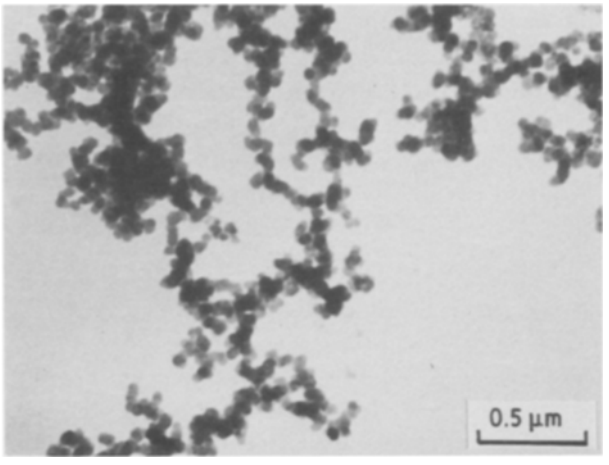

Figure 5 Transmission electron micrograph of $Ni_{0.5}Zn_{0.5}Fe_2O_4$ prepared at 250° C.

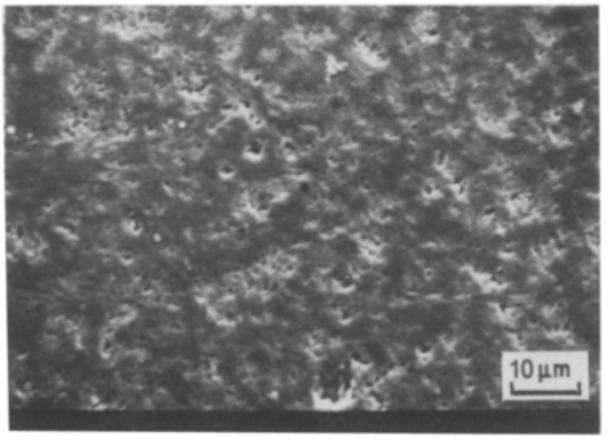

Figure 6 Scanning electron micrograph of polished and chemically etched surface of $Ni_{0.5}Zn_{0.5}Fe_2O_4$ sintered at 1000° C.

4. Conclusions

Ultrafine Ni–Zn ferrites have been prepared by the thermal decomposition/combustion of solid solution precursors $(N_2H_5)_3Ni_xZn_{1-x}Fe_2(N_2H_3COO)_9 \cdot 3H_2O$ where $x = 0.2$ to 0.8. This is probably the first ever report of the preparation of Ni–Zn ferrites not only at low temperatures but also in such fine particles. The importance of fine particles has been in achieving almost theoretical density at low sintering temperatures. The solid solution precursor method is being extended to the preparation of fine particle Mn–Zn ferrites.

Acknowledgements

The authors thank the Department of Science and Technology, Government of India for support of this work.

References

1. E. E. RICHES, in 'Ferrites, A Review of Materials and Applications", edited by J. Gordon Cook (Mills and Boon Limited, London, 1972).
2. J. KULIKOWSKI and A. LESNIEWSKI, *J. of Mag. and Magn. Mater.* **19** (1980) 117.
3. H. IGARASHI and K. OKAZAKI, *J. Amer. Ceram. Soc.* **60** (1977) 51.
4. B. K. DAS, in "Preparation and characterization of Materials", edited by J. M. Honig and C. N. R. Rao (Academic Press, New York, 1981) p. 75.
5. A. GOLDMAN, *Bull. Amer. Ceram. Soc.* **63** (1984) 582.
6. P. RAVINDRANATHAN and K. C. PATIL, *Am. Ceram. Soc. Bull.* **66** (1987) 688.
7. K. C. PATIL, *Proc. Indian Acad. Sci. (Chem. Sci.)* **96** (1986) 459.
8. P. RAVINDRANATHAN and K. C. PATIL, *ibid.* **95** (1985) 345.
9. C. McCRORY-JOY and D. C. JOY, *Talanta* **30** (1983) 299.
10. A. I. VOGEL, "A text book of Quantitative Inorganic Analysis" (Longman Group Limited, London, 1975).
11. K. C. PATIL, R. SOUNDARARAJAN and E. P. GOLDBERG, *Synth. React. Inorg. Met.-Org. Chem.* **13** (1983) 29.
12. A. BRAIBANTI, A. M. MANOTTI LANFREDI, M. A. PELLINGHELLI and E. LEPORATI, *Inorg. Chem.* **7** (1968) 1430.
13. A. BRAIBANTI, A. M. MANOTTI LANFREDI and A. TIRIPICCHIO, *Z. Krist.* **124** (1967) 335.
14. Powder Diffraction File Inorganic Vol. PDIS-10iRB (Joint Committee on Diffraction Standards, Pennsylvania, 1967) pp. 8–234.
15. J. SMIT and H. P. J. WIJN, "Ferrites" (Philips Technical Library, Netherlands, 1959).
16. H. P. KLUG and L. E. ALEXANDER, in "X-ray Diffraction Procedures" (Wiley, New York, 1954) p. 504.
17. D. W. COLLINS, J. T. DEHN and L. N. MULAY, in "Mossbauer Methodology, Vol 3", edited by I. J. Gruvermann (Plenum Press, New York, 1967) p. 103.

Received 14 October 1986
and accepted 22 January 1987